Electronic Supplementary Material (ESI) for New Journal of Chemistry.

Supporting Information

Plasmonic-Based Sensitivity Enhancement of Goos-Hänchen Shift Biosensor Using Transition Metal Dichalcogenides: A Theoretical Insight

Yan Guo[*ab], Nishtha Manish Singh[c], Chandreyee Manas Dasb[c], Qingling Ouyang[bc], Lixing Kang[bc], Kuanbiao Li[d], Philippe Coquet[be], and Ken-Tye Yong[*bc]

[a] School of Automation, Hangzhou Dianzi University, Hangzhou 310018, Zhejiang, China

guoyan@hdu.edu.cn

[b] CINTRA CNRS/NTU/THALES, UMI 3288, Research Techno Plaza, 50 Nanyang Drive, Border X Block, Singapore, 637553

ktyong@ntu.edu.sg

[c] School of Electrical and Electronic Engineering, Nanyang Technological University, 50 Nanyang Avenue, Singapore, 639798

[d] HANGZHOU HANGYANG Co. Ltd, Hangzhou 310014, Zhejiang, China

[e] Institut d'Electronique, de Microélectronique et de Nanotechnologie (IEMN), CNRS UMR 8520 -Université de Lille 1, 59650 Villeneuve d' Ascq, France

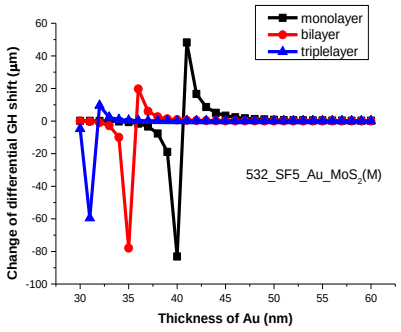
monolayer
bilayer
triplelayer
532_SF5_Au_MoS2(M)
Change of differential GH shift (μm)
Thickness of Au (nm)

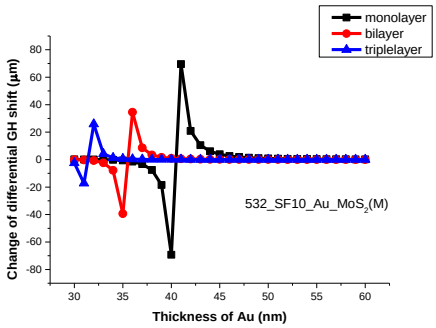
monolayer
bilayer
triplelayer
532_SF10_Au_MoS2(M)
Change of differential GH shift (μm)
Thickness of Au (nm)

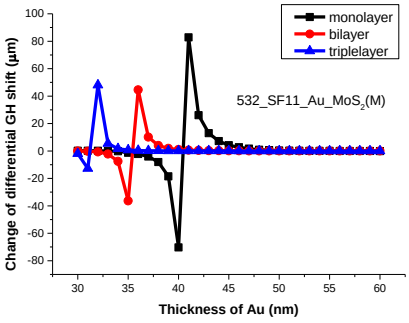
monolayer
bilayer
triplelayer
532_SF11_Au_MoS2(M)
Change of differential GH shift (μm)
Thickness of Au (nm)

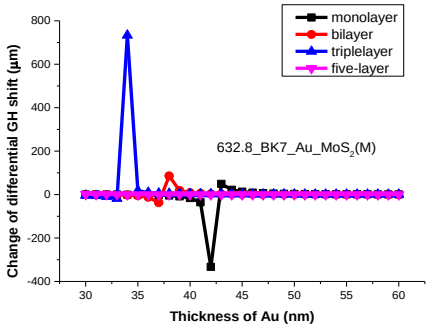
monolayer
bilayer
triplelayer
five-layer
632.8_BK7_Au_MoS2(M)
Change of differential GH shift (μm)
Thickness of Au (nm)

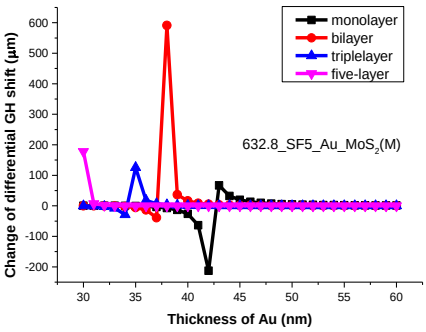
monolayer
bilayer
triplelayer
five-layer
632.8_SF5_Au_MoS2(M)
Change of differential GH shift (μm)
Thickness of Au (nm)

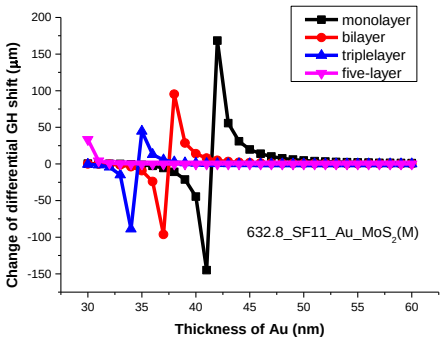
monolayer
bilayer
triplelayer
five-layer
632.8_SF11_Au_MoS2(M)
Change of differential GH shift (μm)
Thickness of Au (nm)

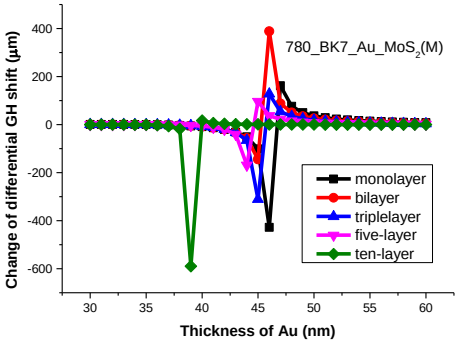
780_BK7_Au_MoS2(M)
monolayer
bilayer
triplelayer
five-layer
ten-layer
Change of differential GH shift (μm)
Thickness of Au (nm)

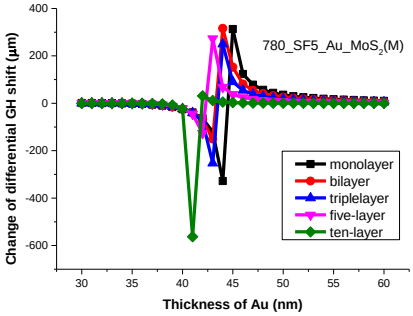
780_SF5_Au_MoS2(M)
monolayer
bilayer
triplelayer
five-layer
ten-layer
Change of differential GH shift (μm)
Thickness of Au (nm)

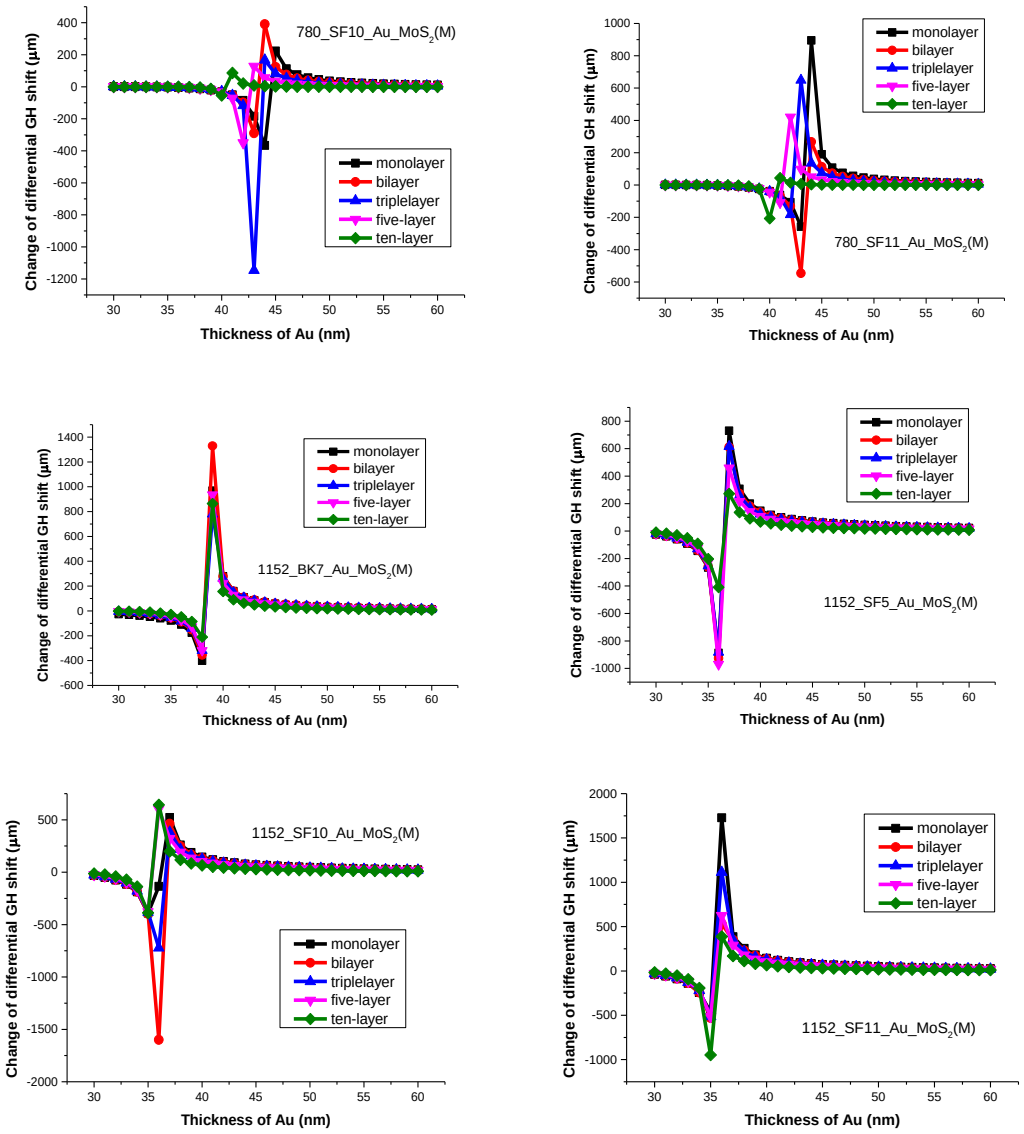

Fig. S1 The change in differential GH shift as a function of the thickness of gold thin film for different number of MoS_2 layers but without graphene (L=0) at different excitation wavelengths coupled by the four prisms.

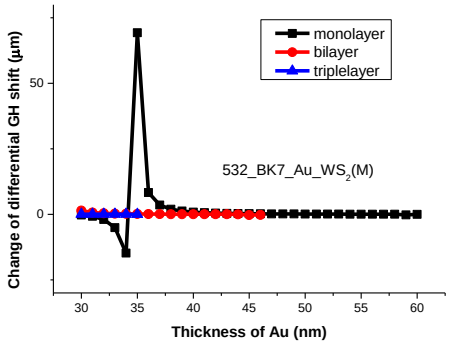
monolayer
bilayer
triplelayer
532_BK7_Au_WS2(M)
Change of differential GH shift (μm)
Thickness of Au (nm)

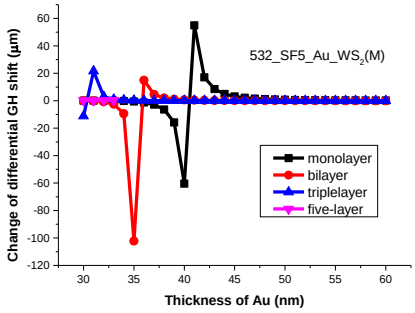
532_SF5_Au_WS2(M)
monolayer
bilayer
triplelayer
five-layer
Change of differential GH shift (μm)
Thickness of Au (nm)

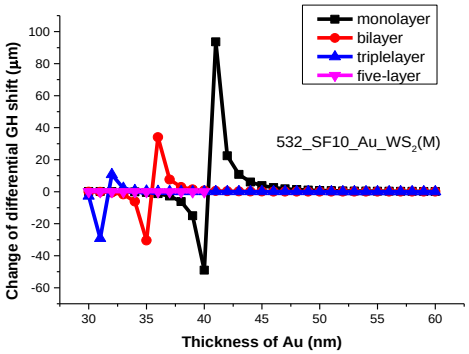
monolayer
bilayer
triplelayer
five-layer
532_SF10_Au_WS2(M)
Change of differential GH shift (μm)
Thickness of Au (nm)

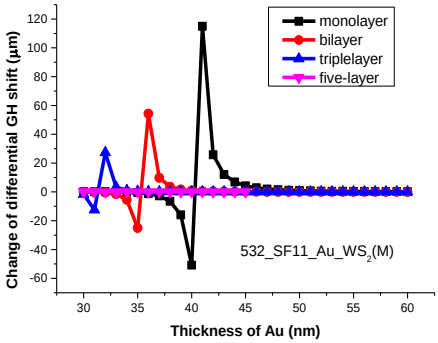
monolayer
bilayer
triplelayer
five-layer
532_SF11_Au_WS2(M)
Change of differential GH shift (μm)
Thickness of Au (nm)

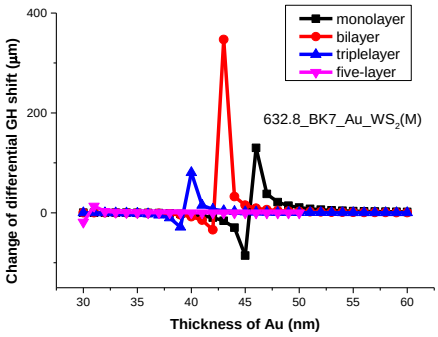
monolayer
bilayer
triplelayer
five-layer
632.8_BK7_Au_WS2(M)
Change of differential GH shift (μm)
Thickness of Au (nm)

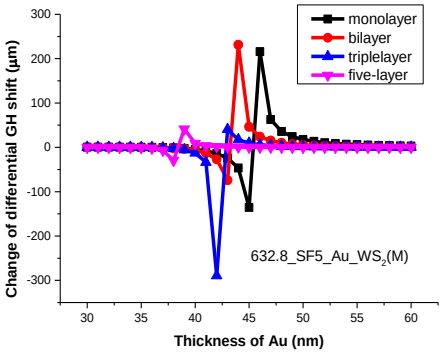
monolayer
bilayer
triplelayer
five-layer
632.8_SF5_Au_WS2(M)
Change of differential GH shift (μm)
Thickness of Au (nm)

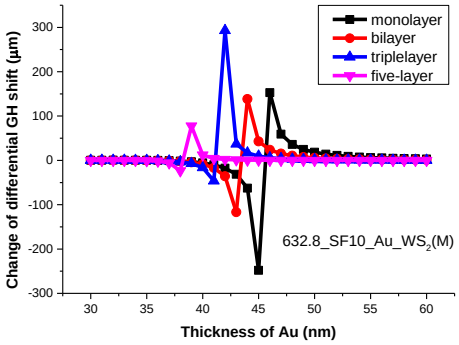
monolayer
bilayer
triplelayer
five-layer
632.8_SF10_Au_WS2(M)
Change of differential GH shift (μm)
Thickness of Au (nm)

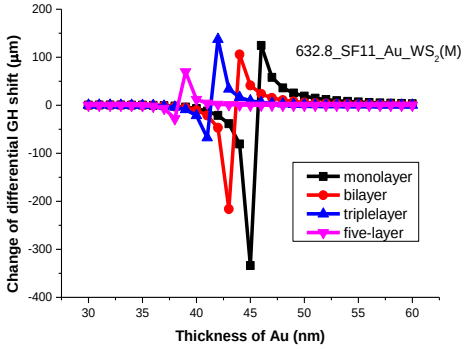
632.8_SF11_Au_WS2(M)
monolayer
bilayer
triplelayer
five-layer
Change of differential GH shift (μm)
Thickness of Au (nm)

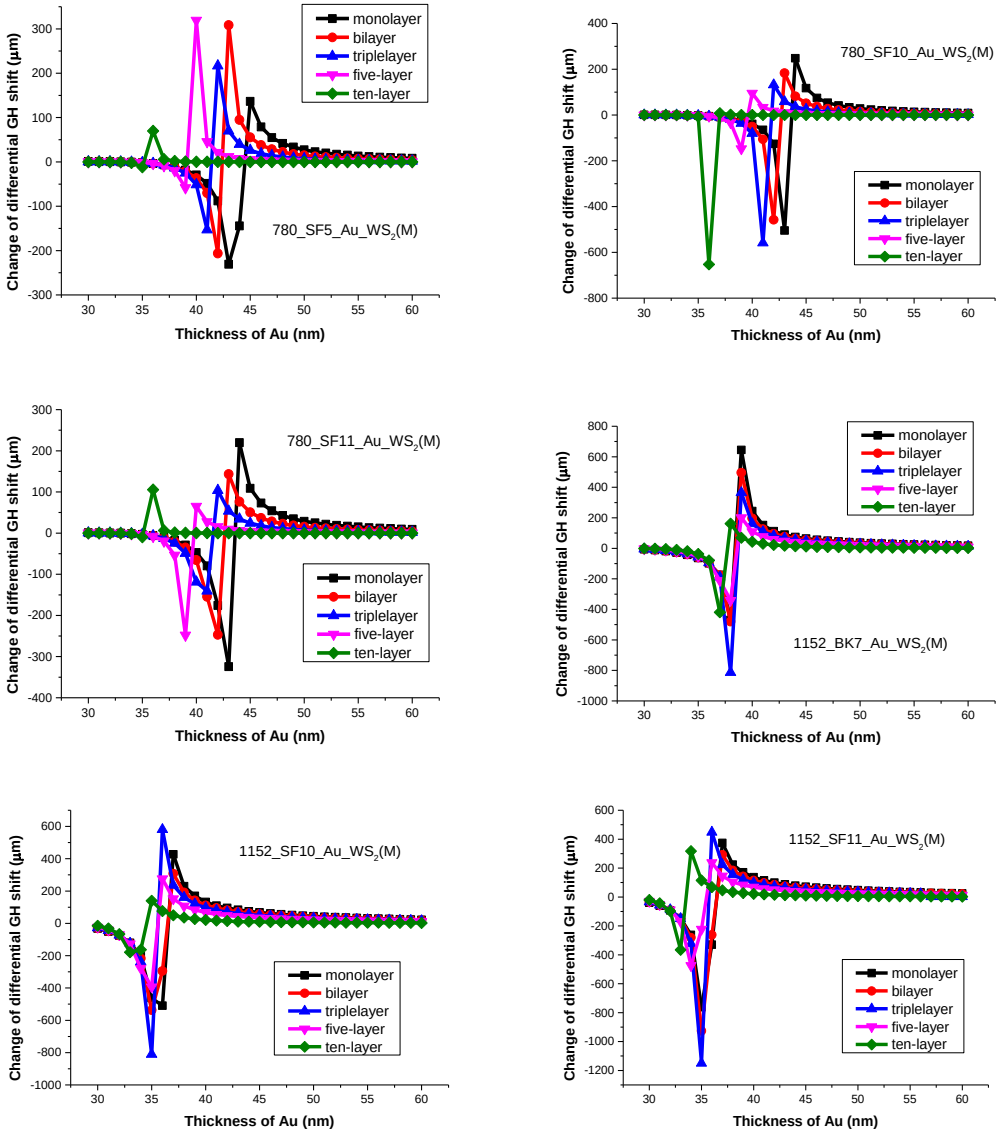

Fig. S2 The change in differential GH shift as a function of the thickness of gold thin film for different number of WS_2 layers but without graphene (L=0) at different excitation wavelengths coupled by the four prisms.

Table S1 Measured parameters- SPR angle, minimum reflectivity, FWTM, change in differential GH shift, sensitivity, FoM and enhancement factor- at the optimal Au thickness with different layers of graphene and MoS_2 at different prisms and excitation wavelengths for the fixed RI change of Δn=0.005.

Fixed Parameters					Measured Parameters						
λ (nm)	Prism	d (nm)	Graphene (L)	MoS_2 (M)	θ_{SPR} (°)	R_{min}	FWTM	|ΔGHs| (μm)	S (μm/RIU)	FoM (×10^4)	η
532	BK7	30	3	1	80.49	1×10^{-6}	5.21	420	8.4×10^4	1.6	5.53
632.8	SF5	42	0	1	60.47	4.1×10^{-7}	1.58	841	1.682×10^5	10.65	2.40
632.8	SF5	38	0	2	61.76	5×10^{-6}	2.74	591	1.182×10^5	4.31	1.68
632.8	SF5	31	4	3	65.10	1×10^{-6}	5.88	678	1.356×10^5	2.31	1.93
632.8	SF10	34	6	1	59.42	1×10^{-6}	3.37	1014	2.028×10^5	6.02	3.34
632.8	SF10	30	5	3	62.33	1×10^{-6}	6.23	648	1.296×10^5	2.08	2.14
632.8	SF11	36	4	1	55.99	2×10^{-6}	2.62	878	1.756×10^5	6.7	1.74
632.8	SF11	40	1	1	55.09	7×10^{-6}	1.73	834	1.668×10^5	9.64	1.65
780	BK7	44	1	2	68.58	2.4×10^{-5}	1.46	632	1.264×10^5	8.66	1.77
780	BK7	41	3	3	70.10	7×10^{-6}	2.20	692	1.384×10^5	6.29	1.94
780	BK7	39	0	10	80.85	1×10^{-6}	4.89	589	1.178×10^5	2.41	1.65
780	SF10	31	12	1	57.30	3×10^{-6}	3.12	664	1.328×10^5	4.26	1.84
780	SF10	41	2	1	55.18	5×10^{-6}	1.01	579	1.158×10^5	11.47	1.61
780	SF10	34	8	2	57.05	5×10^{-6}	2.47	721	1.442×10^5	5.84	2.00
780	SF10	35	7	2	56.80	1×10^{-6}	2.21	1353	2.706×10^5	12.24	3.75
780	SF10	36	6	2	56.56	7×10^{-6}	1.97	961	1.922×10^5	9.76	2.61
780	SF10	38	4	2	56.12	7×10^{-6}	1.57	1167	2.334×10^5	14.87	3.24
780	SF10	43	0	3	55.86	1.6×10^{-5}	1.05	1146	2.292×10^5	21.83	3.18
780	SF10	33	9	3	58.12	4×10^{-6}	3.21	671	1.342×10^5	4.18	1.86
780	SF10	39	3	3	56.53	5×10^{-6}	1.61	1048	2.096×10^5	13.02	2.91
780	SF10	30	13	5	61.75	1×10^{-6}	6.26	628	1.256×10^5	2.0	1.74
780	SF11	44	0	1	52.45	4.2×10^{-5}	0.68	895	1.79×10^5	26.32	2.17
780	SF11	30	13	1	55.02	1×10^{-6}	3.25	1285	2.57×10^5	7.91	3.11
780	SF11	34	8	1	53.89	3×10^{-6}	1.96	1524	3.048×10^5	15.55	3.69
780	SF11	38	4	1	55.13	7×10^{-6}	1.26	906	1.812×10^5	14.38	2.19
780	SF11	42	1	1	52.62	1.9×10^{-5}	0.82	970	1.94×10^5	23.66	2.35
780	SF11	43	0	3	53.40	3.4×10^{-5}	0.94	649	1.298×10^5	13.81	1.57
780	SF11	34	7	5	56.74	3×10^{-6}	3.45	804	1.608×10^5	4.66	1.94
1152	SF5	31	7	1	55.77	1×10^{-5}	1.04	2203	4.406×10^5	42.37	2.88
1152	SF5	34	3	1	55.40	8×10^{-6}	0.73	1956	3.912×10^5	53.59	2.55
1152	SF5	34	3	2	55.54	2.8×10^{-5}	0.78	1952	3.904×10^5	50.05	2.55
1152	SF5	31	7	3	56.11	5×10^{-6}	1.19	2576	5.152×10^5	43.29	3.36
1152	SF5	33	4	5	56.15	3×10^{-6}	1.04	1566	3.132×10^5	30.12	2.04
1152	SF5	31	7	10	57.69	1×10^{-6}	1.91	1630	3.26×10^5	17.07	2.13
1152	SF11	36	0	1	50.61	7.7×10^{-5}	0.47	1728	3.456×10^5	73.53	1.54
1152	SF11	31	6	1	51.08	3×10^{-6}	0.84	2694	5.388×10^5	64.14	2.41
1152	SF11	34	2	3	51.01	6×10^{-6}	0.66	2257	4.514×10^5	68.39	2.02
1152	SF11	33	3	3	51.10	3.7×10^{-5}	0.74	1760	3.52×10^5	47.57	1.57
1152	SF11	33	3	5	51.39	4×10^{-6}	0.84	2132	4.264×10^5	50.76	1.91

Table S2 Measured parameters- SPR angle, minimum reflectivity, FWTM, changes in differential GH shift, sensitivity, FoM and enhancement factor- at the optimal Au thickness along with different layers of graphene and WS_2 at different prisms and excitation wavelengths for the fixed RI change of $\Delta n=0.005$.

Fixed Parameters					Measured Parameters						
λ (nm)	Prism	d (nm)	Graphene (L)	WS_2 (M)	θ_{SPR} (°)	R_{min}	FWTM	|ΔGHs| (μm)	S (μm/RIU)	FoM (×10^4)	η
532	BK7	31	2	1	81.0	6×10^{-6}	4.99	211	4.22×10^4	0.85	2.78
532	SF11	33	2	2	62.42	1×10^{-6}	5.82	496	9.92×10^4	1.7	1.43
632.8	SF5	39	2	3	65.17	4×10^{-6}	3.63	463	9.26×10^4	2.55	1.32
632.8	SF10	35	7	1	59.98	1×10^{-7}	3.49	1059	2.118×10^5	6.67	3.50
632.8	SF11	36	5	2	58.11	1×10^{-6}	3.51	1724	3.448×10^5	9.82	3.41
780	BK7	40	4	1	68.80	1×10^{-6}	1.95	1729	3.458×10^5	17.73	4.86
780	BK7	33	11	2	72.33	1×10^{-7}	4.49	870	1.74×10^5	3.88	2.44
780	BK7	43	1	2	69.14	9×10^{-6}	1.71	918	1.836×10^5	10.74	2.58
780	SF10	41	0	3	56.51	3.1×10^{-5}	1.43	559	1.118×10^5	7.82	1.55
780	SF10	36	0	10	70.82	1×10^{-7}	8.51	652	1.304×10^5	1.53	1.81
780	SF10	38	4	1	55.73	1.5×10^{-5}	1.41	688	1.376×10^5	9.76	1.91
780	SF10	39	3	1	55.54	7×10^{-6}	1.25	1323	2.646×10^5	21.17	3.68
780	SF10	36	5	2	56.81	7×10^{-6}	2.08	665	1.33×10^5	6.39	1.85
780	SF10	30	12	3	60.16	1×10^{-7}	5.31	539	1.078×10^5	2.03	1.50
780	SF11	42	0	2	53.24	5×10^{-6}	1.00	813	1.626×10^5	16.26	1.97
780	SF11	41	0	3	54.0	1.6×10^{-5}	1.32	689	1.378×10^5	10.44	1.67
780	SF11	40	2	1	52.94	1.3×10^{-5}	1.02	1345	2.69×10^5	26.37	3.25
780	SF11	30	12	2	56.14	1×10^{-7}	4.05	1613	3.226×10^5	7.97	3.91
780	SF11	38	3	2	53.85	4×10^{-6}	1.51	850	1.7×10^5	11.26	2.06
780	SF11	34	5	5	57.91	1×10^{-6}	4.25	873	1.746×10^5	4.11	2.11
1152	BK7	34	6	1	64.57	2×10^{-6}	1.21	2735	5.47×10^5	45.21	1.61
1152	BK7	36	3	2	64.51	6×10^{-6}	1.03	2961	5.922×10^5	57.5	1.74
1152	SF5	36	0	3	55.59	4.4×10^{-5}	0.70	1449	2.898×10^5	41.4	1.89
1152	SF5	33	4	1	55.55	1×10^{-6}	0.83	3035	6.07×10^5	73.13	3.96
1152	SF5	35	1	2	55.49	3×10^{-5}	0.70	1475	2.95×10^5	42.14	1.92
1152	SF5	30	8	3	56.46	4×10^{-6}	1.45	2726	5.452×10^5	37.6	3.56
1152	SF5	33	3	5	56.42	4×10^{-6}	1.18	2713	5.426×10^5	45.98	3.54
1152	SF11	33	3	1	50.89	9×10^{-6}	0.68	2264	4.528×10^5	66.59	2.02
1152	SF11	32	4	2	51.16	2.4×10^{-5}	0.82	1889	3.778×10^5	46.07	1.69

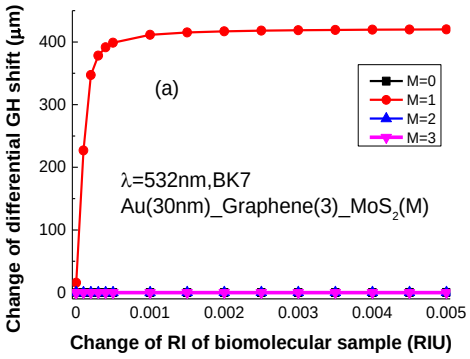

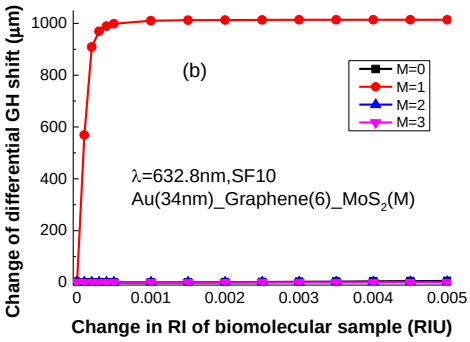

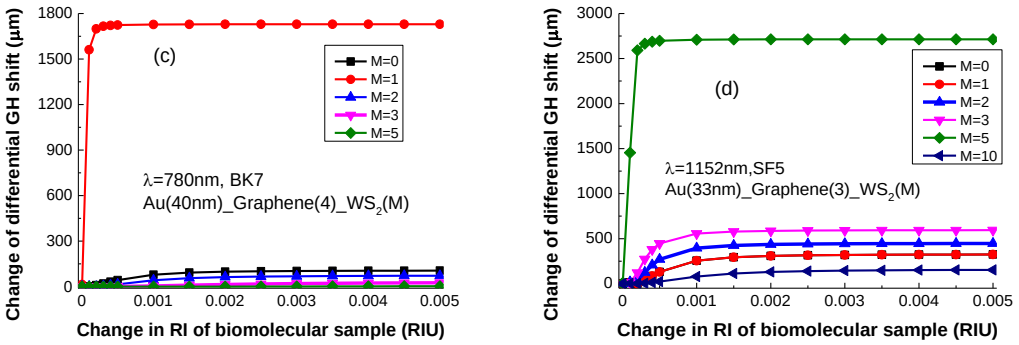

Fig. S3 Optimization the layer numbers of MS_2 to achieve large differential GH shift change with respect to the RI change of biomolecular samples for the four configurations.

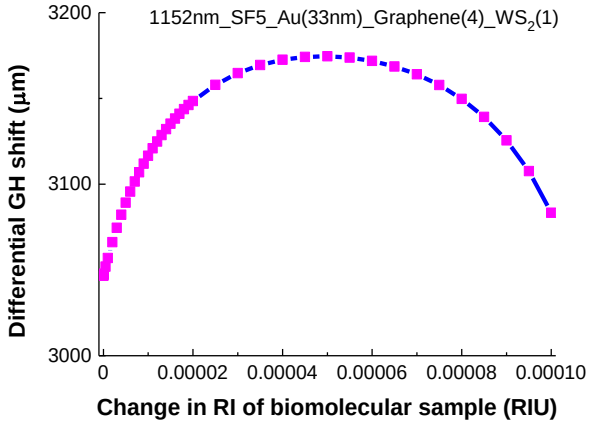

Fig. S4 Differential GH shift GHs with respect to the RI change of biomolecular solutions for the configuration of monolayer WS_2 with four-layer graphene structured on 33 nm Au illuminated by 1152 nm coupled by SF5 prism.